Available online at www.sciencedirect.com
ScienceDirect
Journal of Hazardous Materials 147 (2007) 1020–1027
Journal of Hazardous Materials
www.elsevier.com/locate/jhazmat

Physical and chemical properties and adsorption type of activated carbon prepared from plum kernels by NaOH activation

Ru-Ling Tseng *

Department of Safety, Health and Environmental Engineering, National United University, Miao-Li 360, Taiwan

Received 7 October 2006; received in revised form 13 December 2006; accepted 27 January 2007
Available online 6 February 2007

Abstract

Activated carbon was prepared from plum kernels by NaOH activation at six different NaOH/char ratios. The physical properties including the BET surface area, the total pore volume, the micropore ratio, the pore diameter, the burn-off, and the scanning electron microscope (SEM) observation as well as the chemical properties, namely elemental analysis and temperature programmed desorption (TPD), were measured. The results revealed a two-stage activation process: stage 1 activated carbons were obtained at NaOH/char ratios of 0–1, surface pyrolysis being the main reaction; stage 2 activated carbons were obtained at NaOH/char ratios of 2–4, etching and swelling being the main reactions. The physical properties of stage 2 activated carbons were similar, and specific area was from 1478 to 1887 $m^2\ g^{-1}$. The results of reaction mechanism of NaOH activation revealed that it was apparently because of the loss ratio of elements C, H, and O in the activated carbon, and the variations in the surface functional groups and the physical properties. The adsorption of the above activated carbons on phenol and three kinds of dyes (MB, BB1, and AB74) were used for an isotherm equilibrium adsorption study. The data fitted the Langmuir isotherm equation. Various kinds of adsorbents showed different adsorption types; separation factor (R_L) was used to determine the level of favorability of the adsorption type. In this work, activated carbons prepared by NaOH activation were evaluated in terms of their physical properties, chemical properties, and adsorption type; and activated carbon PKN2 was found to have most application potential.

Keywords: Activated carbons; NaOH-activation; Physical properties; Chemical properties; Adsorption type

1. Introduction

Activated carbon is a widely used adsorbent in the treatment of wastewater and drinking water. Adsorption type and capacity are primarily based on the physical properties of the pores, namely the specific surface area, the pore size and distribution. Measurement of adsorption and desorption of N_2 at 77 K and scanning electron microscope (SEM) observation provided important pore characteristics; then the adsorption type and capacity of the activated carbon could be evaluated. The data of adsorption and desorption isotherm of N_2 at 77 K are the most investigated physical property of activated carbon. This measurement has been used in 89% related to activated carbon prepared from raw plant material in 2005. These data provide not only specific area (S_p), total pore volume (V_{pore}), and pore size distribution but are also used to calculate micropore volume and exterior surface area (S_{ext}). Studying the shapes of the isotherm curve and hysteresis can be used to infer distribution, shape and structure of the pores inside activated carbon. This measurement is a prerequisite. Differences in surface structure features of activated carbon prepared from various raw materials, activation methods and conditions can be investigated with SEM observation. Surface features of activated carbon prepared under various conditions were observed in the previous studies [1,2]. The results were used in inferring the activation reaction mechanism.

Factors affecting adsorption type are pore structure, surface chemistry, and adsorbent properties. Among them functional groups and chemical compositions play important roles in the adsorption mechanism and capacity. Measurements of elemental analysis and temperature programmed desorption can be employed for understanding chemical properties of activated carbon. Chemical compositions of activated carbon were measured with elemental analysis by some investigators [3–5].

* Tel.: +886 37 381775; fax: +886 37 333187.
E-mail address: trl@nuu.edu.tw.

0304-3894/$ – see front matter © 2007 Elsevier B.V. All rights reserved.
doi:10.1016/j.jhazmat.2007.01.140

Literature reveals little about relationships between the chemical compositions of activated carbon and its preparation conditions as well as activation mechanisms. The changes in the chemical compositions of the material during the activation process cannot be completely described. Thus, investigation of the chemical compositions of activated carbon with elemental analysis is important. Temperature programmed desorption (TPD) can be utilized to determine the strength of the surface active groups, quantity, and type of activated carbon. Stones prepared activated carbons by steam and CO_2 activation [6]. Carbons were desorbed with TPD and the functional groups (carbonyl, carboxylic, phenolic, etc.) were investigated. Wu et al. [7] prepared activated carbon and measured it with TPD. It was found that KOH-activated carbon released more CO_2 than steam-activated carbon did. TPD measurement is getting more important in the field of activated carbon research.

Recently, NaOH activation, which reduces chemical activation cost and environmental load, has gradually been drawing more attention from researchers [8–13]; but studies have been limited to coal as raw material. Activated carbon prepared from plant material is higher of O/C and H/C ratios and its physical properties, chemical properties, and adsorption type are significantly different from those prepared from coal. Good effects of activated carbon prepared from hard plum kernels were found in the previous studies [14,15]. Thus, in this study, high surface area activated carbon was prepared from plum kernels by NaOH activation, having a lower environmental load. The physical properties (adsorption and desorption isotherm of N_2 at 77 K and scanning electron microscope) and the chemical properties (elemental analysis and temperature programmed desorption) of activated carbon were measured. Adsorption on dyes and phenol was used to investigate adsorption type. In order to understand the NaOH activation mechanism of raw plant material, the optimum dosage of NaOH activation had to be evaluated.

2. Materials and methods

2.1. NaOH activation

In this study, the plum kernels were pretreated at 110 °C for more than 24 h until dry and then put into a high temperature oven, which was kept oxygen-starved by introducing nitrogen gas. The oven was kept at 450 °C for 2 h to carbonize the plum kernels. The carbonization yield of plum kernels was 37.0 wt.%.

The char was ground and sieved and the part with a particle size between 0.833 and 1.65 mm was activated. The activation was done by dissolving some NaOH in water to which the char was added, uniformly mixed, dried at 130 °C, and then placed in a high temperature oven. Nitrogen gas was introduced into the oven. The oven was heated to 780 °C and kept there for 1 h. The product was neutralized with equal NaOH equivalents of HCl solution (600 cm^3) till the disappearance of most of the CO_2 bubbles, then a large amount of 10% HCl solution was added, it was water bathed at 80 °C for 1 h, after which washing was continued with distilled water till the pH of the water was neutral. The samples were classified according to agent/char ratio as PKN0, PKN0.5, PKN1, PKN2, PKN3, and PKN4. The first two characters, PK, represent the plum kernels; the third character, N, represents NaOH activation; the last number represents the weight NaOH/char ratio.

2.2. Measurement of pore structure

Burn-off was defined as the ratio of weight of carbon left after carbonization weight loss of the activated carbon. The BET surface area was obtained from 77 K N_2 isotherm adsorption with a sorptiormeter (Porous Materials, BET-202A). The adsorption data of the total pore volume (V_{pore}) were obtained from calculating with the manufacturer's software. Pore size distribution was inferred using the BJH theory (Barrett, Joyner and Halendya) [16]. The *t*-polt method was used to calculate the micropore volume (V_{micro}) and the exterior surface area (S_{ext}) [17,18]. The micropore surface area (S_{micro}) was obtained from S_p minus S_{ext} [19].

2.3. SEM observation

Activated carbon with particle size between 40 and 80 mesh was obtained from the sieving. The particles were stuck on to the measuring tube with carbon glue, gold-plated with a vacuum electroplating machine for about 60 s, and then observed with SEM (JSM-5600 JEOL Co.).

2.4. Elemental analysis

The sample was uniformly ground, oven-dried at 130 °C overnight. A sample of 3.0 mg was analyzed in an aluminum box. The sample was analyzed three times with an elemental analyzer (Elemental Analyzer, Model 611B, CH Instruments). Adjustment analysis with a standard sample of sulfanilic acid was carried out in parallel with an ordinary sample analysis.

2.5. Temperature programmed desorption

Activated carbon was oven-dried at 130 °C overnight, weighted, and placed in a U shape reactor. He gas was introduced into the reactor at 30 $cm^3\ min^{-1}$. The thermal conductive detector (TCD) was set at 150 °C. After the instrument was stable, the temperature rising program was stared; the temperature rose from room temperature to 800 °C in 50 min. An information-collecting machine was employed to read and take the data.

2.6. Procedures for adsorption experiments

Four solutes including acid blue 74 (AB74), basic brown 1 (BB1), methylene blue (MB), and phenol, all from Merck Co., were used. Molecular weights were, respectively, 466.4, 419.4, 284.3, and 94.1 $g\ mol^{-1}$. The molecular weight of MB does not include associated chloride ion. The adsorption experiments were the same as those detailed in literatures [20,21].

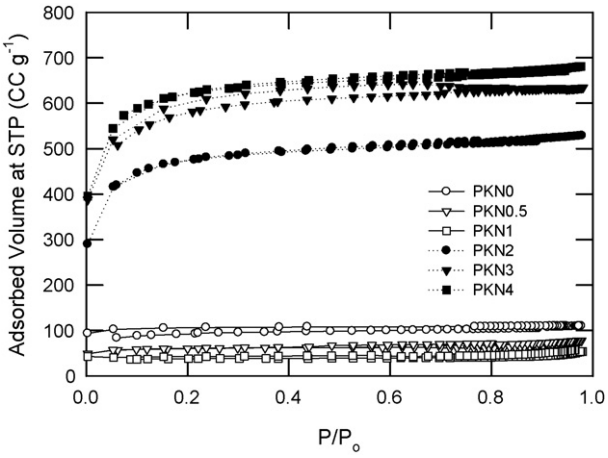

Fig. 1. Adsorption/desorption isotherms of N_2 at 77 K on activated carbon derived from plum kernels by NaOH activation (carbons are PKN0 (◯), PKN0.5 (▽), PKN1 (□), PKN2 (●), PKN3 (▼), and PKN4 (■), respectively).

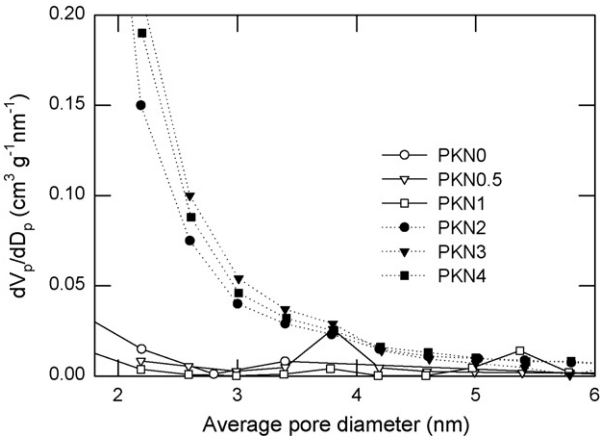

Fig. 2. Pore size distribution of the activated carbon derived from plum kernels by NaOH activation (carbons are PKN0 (◯), PKN0.5 (▽), PKN1 (□), PKN2 (●), PKN3 (▼), and PKN4 (■), respectively).

3. Results and discussion

3.1. Physical properties of activated carbon

Before designing and using the adsorption process, the pore structure of the adsorbent must be done [18,22]. Fig. 1 shows the curves of the 77 K N_2 isotherm adsorption/desorption of the activated carbon obtained at six different values of the NaOH/char ratio in this study. Values of NaOH/char ratio of stage 1 activated carbon were from 0 to 1 (empty circles in the figure); those of stage 2 were from 2 to 4 (solid circles in the figure). Fig. 1 shows that the adsorption volume of stage 1 activated carbons did not significantly change when the values of P/P_0 were increased from minimum to maximum, the pores are mostly straight tubes [23]. The adsorption volume of this type of activated carbons was low. For stage 2 activated carbon, the adsorption volumes of PKN3 and PKN4 were almost the same (=391 $cm^3\ g^{-1}$), that of PKN2 somewhat lower. The adsorption volumes of these three activated carbons increased rapidly when P/P_0 was first increased, then increased mildly, and then increased least after $P/P_0 > 0.2$. The tendencies of these three curves are similar, i.e. they have similar pore size distributions.

Fig. 2 shows the pore sizes distributions. The pore sizes of stage 1 activated carbon were mostly smaller than 2 nm; while those of stage 2 were mostly smaller than 3 nm and gradually disappeared for pore sizes larger than 5 nm.

Table 1 lists the physical properties of activated carbon derived from plum kernels by NaOH activation. The data show that the S_p value of stage 1 activated carbons decreased from 290 to 113 $m^2\ g^{-1}$ when the NaOH/char ratio increased from 0 to 1; this is different from that of carbon activated with KOH [2]. However, the S_p value of this type of activated carbon is too small. For the time being, they seem to be of no practical value. However, investigating the activation mechanism and understanding this phenomenon are quite meaningful. The values of S_p and V_p of PKN2, PKN3, and PKN4, stage 2 activated carbons, increased with an increased NaOH/char ratio, from 1478 to 1887 $m^2\ g^{-1}$ and 0.815 to 1.049 $cm^3\ g^{-1}$, respectively. However, their porosity (ε), micropore ratio (V_{micro}/V_p), and Burn-off hardly increased, from 0.642 to 0.698, 0.82 to 0.86, and 0.77 to 0.80, respectively. The average pore sizes (D_p) were 2.2 nm, revealing the similar physical properties among these three samples of activated carbon.

Relationships between the pore characteristics of the activated carbon and the NaOH/char ratio are shown in Fig. 3a–d; stage 1 activated carbon is represented by empty circles: stage 2 activated carbon by solid circles. Specific area, pore volume, and micropore ratio of stage 1 activated carbon decreased with increased NaOH/char ratio; burn-off of PKN0 was 0.5, and of PKN0.5 and PKN1 0.71 and 0.72, respectively. This means that burn-off of PKN0.5 had reached a new equilibrium zone. Specific area, pore volume, and micropore ratio of stage 2 activated

Table 1
Physical properties of carbon derived from plum kernels by NaOH activation

Carbons	S_p ($m^2\ g^{-1}$)	V_p ($cm^3\ g^{-1}$)	ε[a] (−)	V_{micro}/V_p	D_p[b] (nm)	Burn-off	ρ_b[c] ($kg\ m^{-3}$)
PKN0	290	0.169	0.272	0.77	2.3	0.50	0.611
PKN0.5	183	0.120	0.209	0.73	2.6	0.71	0.561
PKN1	113	0.083	0.155	0.63	2.9	0.72	0.517
PKN2	1478	0.815	0.642	0.82	2.2	0.77	0.327
PKN3	1772	0.977	0.683	0.85	2.2	0.80	0.229
PKN4	1887	1.049	0.698	0.86	2.2	0.79	0.266

[a] Porosity (ε) = $V_p/[V_p + (1/\rho_s)]$.
[b] Average pore diameter (D_p) = $4V_p/S_p$.
[c] Bulk density(ρ_b).

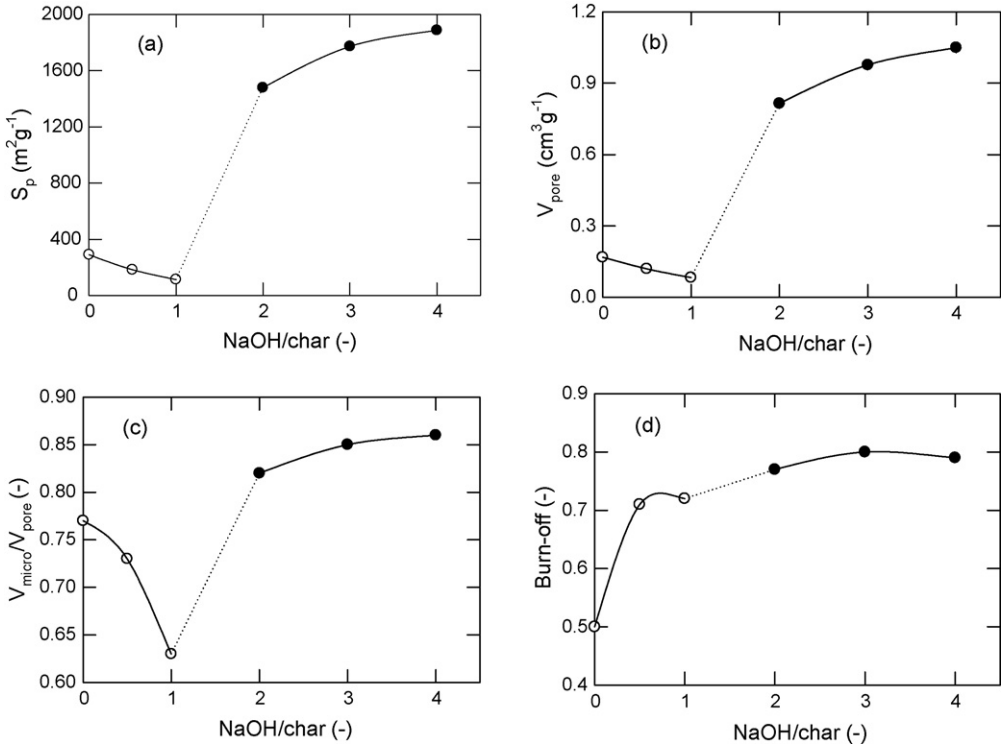

Fig. 3. (a) BET surface area (S_p), (b) total pore volume (V_p), (c) micropore volume rate (V_{micro}/V_p), and (d) burn-off of activated carbon at different NaOH/char ratios.

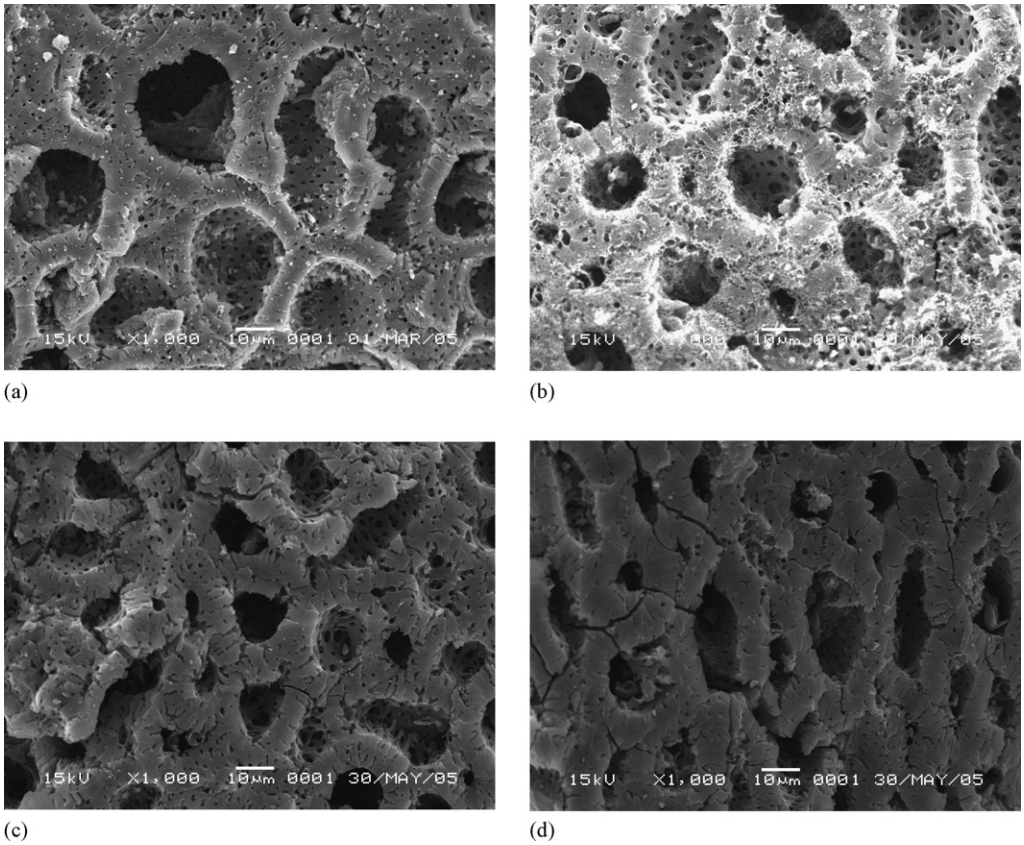

Fig. 4. SEM photos: (a) PKN0, (b) PKN1, (c) PKN2, and (d) PKN4.

carbon increased significantly, meaning that a different reaction mechanism had been triggered; and their burn-off was still maintained in a near equilibrium zone (0.7–0.8). It is of interest that the S_p value increased from 183 to 1887 $m^3\ g^{-1}$ in the burn-off equilibrium zone (PKN0.5 to PKN4); a huge variation. This is like making loose cakes of different porosities from the same quantity of flour; stage 1 activated carbon can be thought of as a dense cake of an unsuccessfully fermented product, while stage 2 carbon, as lose well-fermented cakes. So, specific area, pore volume, and micropore ratio of Fig. 3 appear to have a tendency to increase with increased NaOH/char ratio at stage 2.

3.2. SEM observation

Fig. 4a–d were 1000× magnified SEM photos of the activated carbon. Fig. 4a shows that PKN0 had some large holes and walls within which there were many tiny holes, surface pyrolysis being the primary reaction in the activation process. PKN1, in Fig. 4b, showed severe erosion on the mouths of both the huge and tiny holes within walls. Surface pyrolysis and NaOH etching occurred in the activation process, but only on the surface. Thus, the BET specific surface area and the total pore volume decreased, resulting in a decreased micropore ratio. Fig. 4c and d show compressed and twisted holes walls due to swelling. Swelling in PKN4 was more violent than PKN2, thus the S_p and V_p values of PKN4 were larger.

3.3. Elemental analysis of the chemical properties of activated carbon

In this study, the chemical compositions of activated carbon obtained from elemental analysis are listed in Table 2. PKN0 in Table 2 is in agreement with those stated in the literatures: elements H and O of botanic material lose more easily in the heat treatment under oxygen-starved condition [3]. Elements H and O were more easily lost than element C in raw plant material in oxygen-starved pyrolysis.

Loss ratio is defined as the ratio of weight loss of a certain element in char during activation to the weight content of that element in char (X_{char}), which can be calculated as:

$$X\ \text{loss ratio} = \frac{X_{char} - X_{ac}(1 - \text{Burn-off})}{X_{char}} \quad (1)$$

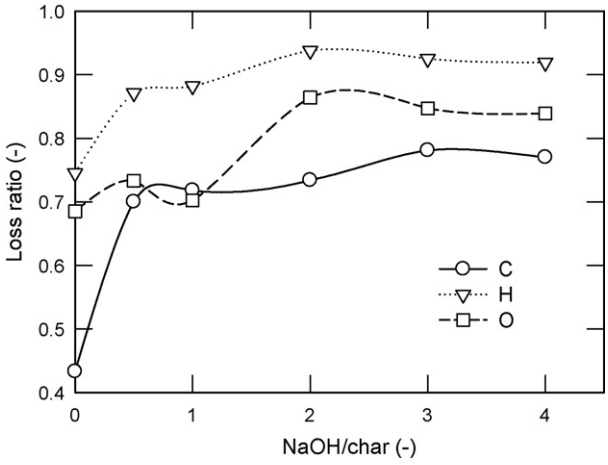

Fig. 5. C, H, and O loss% of activated carbon at different NaOH/char ratios.

where X_{char} is the element X weight content in char and X_{ac} is the element X weight content in the activated carbon.

X can be any one element of C, H, and O. Loss ratios of C, H, and O are listed in Table 2. Data in the table show that loss ratios of H and O were higher than that of C; this is the case of raw plant material (char) after pyrolysis; the highest loss ratios of H and O occurred to PKN2; the highest loss ratio of C occurred to PKN3. Fig. 5 shows the relationships between loss ratios of C, H, and the NaOH/char ratio. C loss ratios already reached a new equilibrium zone (0.70–0.78) with PKN0.5; H loss ratio also reached a new equilibrium zone of 0.87–0.95 with PKN0.5. Note that only the O loss ratio curve has a two-stage characteristic: stage 1 loss ratios were between 0.69 and 0.72, while stage 2 loss ratios were between 0.84 and 0.86. This distinction between stages is in accordance with the physical properties of Section 3.1. It can reasonably be inferred that the largely increased values of S_p and V_p of stage 2 activated carbon is because of the increased O loss ratio. Thus, the reaction mechanism can be assumed as:

$$4NaOH + C \longleftrightarrow 4Na + CO_2 + 2H_2O \quad (2)$$

The reaction mechanism was proved to exist as reported in literature [24]. Na production in Eq. (2) joins the following reaction mechanism:

$$2Na \xrightarrow{\text{oxidation}} Na_2O \xrightarrow{\text{hydration}} NaOH \quad (3)$$

Table 2
Chemical compositions of the raw material and activated carbon

Activated carbons	Elemental composition (wt.%)					C loss ratio	H loss ratio	O loss ratio
	C	H	N	S	O_{diff}[a]			
PK-Char	73.80	3.43	0.69	0.12	21.97	0	0	0
PKN0	83.72	1.75	0.63	0.09	13.82	0.433	0.745	0.685
PKN0.5	76.22	1.52	1.17	0.05	21.04	0.700	0.871	0.722
PKN1	74.36	1.44	0.79	0.03	23.38	0.718	0.882	0.702
PKN2	85.23	0.92	0.88	0.02	12.95	0.734	0.938	0.864
PKN3	80.81	1.27	1.08	0.02	16.82	0.781	0.925	0.847
PKN4	80.76	1.31	1.01	0.03	16.89	0.770	0.919	0.839

[a] O_{diff}: the oxygen is assessed by difference.

It can be inferred that the gas produced in formula (2) is the main reason for the swelling of the activated carbon and the increased values of S_p and V_p; formula (3) is the reason for the increased O loss ratio.

It is commonly believed that the mechanism of NaOH activation is according to the following reaction [22]:

$$6NaOH + 2C \longleftrightarrow 2Na + 2Na_2CO_3 + 3H_2 \quad (4)$$

Metal ions also deposited on the cover and walls of the container [10]. However, this cannot fully explain the huge loss ratios of H and O of the raw plant material (char). But, if part of the Na produced in formula (4) subsequently joins the reaction of formula (3), then the increased loss ratios of C, H, and O of PKN0.5 can be explained.

3.4. Temperature programmed desorption of the chemical properties of activated carbon

Inert gas (He) is introduced through the sample surfaces in temperature programmed desorption. Desorption begins as the temperature of the sample rises. At lower temperatures (<550 °C), CO_2 is desorbed because of the existence of anhydrides, lactones, and carboxyl; while the desorption of CO occurs at higher temperatures (above 500 °C) because of the existence of quinine, hydroxyl, and carbonyl groups [25–27]. Thus, distribution of oxygen-containing functional groups can be understood with the TPD results. Fig. 6 shows results of the TPD of the activated carbon studied in this work. Desorption of PKN0 at lower temperatures (<550 °C) and at higher temperatures (>500 °C) are the most; PKN4, next; PKN2, the least. This is in accordance with the H and O of elemental analysis. PKN2 has the least desorption because of its high loss ratios of H and O.

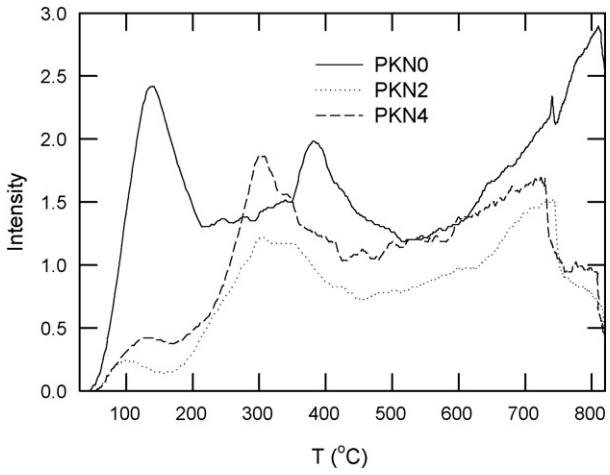

Fig. 6. Evolution profiles of CO_2 and CO by temperature programmed desorption (carbons are PKN0 (—), PKN1 (···), and PKN4 (– – –), respectively).

3.5. Isotherm adsorption

High surface area activated carbon of similar physical and chemical properties (PKN2, PKN3, and PKN4) was employed to study isotherm adsorption on dyes (MB, BB1, and AB74) and phenol in this work. The results are described with the Langmuir isothermal equation as follow:

$$\frac{C_e}{q_e} = \left(\frac{1}{K_L q_{mon}}\right) + \left(\frac{1}{q_{mon}}\right) C_e \quad (5)$$

where C_e and q_e are, respectively, the concentration ($g\,m^{-3}$) and adsorption amount ($g\,kg^{-1}$) at adsorption equilibrium, q_{mon} the amount of adsorption corresponding to monolayer coverage ($g\,kg^{-1}$), and K_L is the Langmuir constant ($m^3\,g^{-1}$). The results are summarized in Table 3. All r^2 values were larger than 0.995, meaning that the data were suitably fitted with the Langmuir isothermal equation. The q_{mon} values of MB adsorption on PKN2, PKN3, and PKN4 were from 765 to 828 $g\,kg^{-1}$; AB74, from 549 to 567 $g\,kg^{-1}$; BB1, from 1453 to 1845 $g\,kg^{-1}$; and phenol, from 269 to 277 $g\,kg^{-1}$. The q_{mon} values of adsorption of MB, AB74, and phenol hardly varied with the change of values of the NaOH/char ratio.

Data of adsorption isotherm equilibrium provide the information not only of adsorption amount, but also for judging the adsorption type. Difference of adsorption types of activated car-

Table 3
Parameters of the Langmuir equation and separation factor in the adsorption of dyes and phenol solutes on various samples of activated carbon at 30 °C

Solute	Adsorbent	Langmuir equation			Favorable parameter, $K_L C_i$	Separation factor, R_L [a]
		q_{mon} ($g\,kg^{-1}$)	K_L ($m^3\,g^{-1}$)	r^2		
MB	PKN2	765	0.560	0.9999	392	
	PKN3	785	0.361	0.9991	253	0.0039
	PKN4	828	0.488	0.9995	341	0.0029
AB74	PKN2	549	0.163	0.9952	65.2	0.0151
	PKN3	561	0.155	0.9961	62.1	0.0158
	PKN4	567	0.216	0.9971	86.2	0.0115
BB1	PKN2	1453	0.049	0.9990	48.6	0.0206
	PKN3	1529	0.049	0.9994	48.6	0.0206
	PKN4	1845	0.030	0.9976	30.2	0.0321
Phenol	PKN2	259	0.043	0.9986	20.4	0.0467
	PKN3	262	0.043	0.9996	20.3	0.0469
	PKN4	277	0.042	0.9951	19.9	0.0478

[a] $R_L = 1/[1 + (K_L C_i)]$.

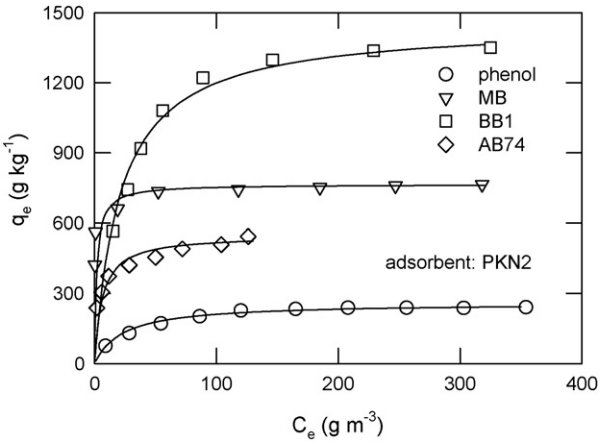

Fig. 7. Adsorption isotherms of dyes and phenol at 30 °C on the PKN2 activated carbon (adsorbates are phenol (◯), MB (▽), BB1 (□), and AB74 (◊), respectively). The solid curves were calculated with the Langmuir equation.

bon adsorption on different adsorbates shown in Fig. 7 can be understood from the following discussion.

Dimensionless separation factor, R_L, can be calculated from the fitted Langmuir isotherm equation to determine the type of adsorption process [28]. Separation factor, R_L, is defined as:

$$R_L = \frac{1}{1 + K_L C_i} \tag{6}$$

or expressed by Favorable parameter, $K_L C_i$, as

$$K_L C_i = \frac{1 - R_L}{R_L} \tag{7}$$

C_i value in formulas (6) and (7) is the initial concentration, the maximum value, of the adsorption process. The relationships of R_L, $K_L C_i$ and type of process are shown in Table 4. The R_L value is classified as: $R_L > 1$ meaning Unfavorable; $0 < R_L < 1$, Favorable; $R_L = 0$, Irreversible. Actually, the R_L values of all adsorbents are between 0 and 1 (Favorable type). In this work, the R_L values of PKN2 adsorption on MB, AB74, BB1, phenol were, respectively, 0.0025, 0.0151, 0.0206, and 0.0467, which would make them a Favorable type. But it is difficult to evaluate Favorable level according to R_L values between 0 and 1. In this paper, Favorable parameter, $K_L C_i$ value, is suggested to use to evaluate the Favorable level, as shown in Table 4. If $K_L C_i$ value is negative, then it is Unfavorable; if positive, Favorable; the larger the $K_L C_i$ value, the higher the Favorable level; if the $K_L C_i$ value approaches infinite, it is an Irreversible process. $K_L C_i$ value can be employed to judge the Favorable level. For example: in this study, the $K_L C_i$ values of PKN2 adsorption on MB, AB74, BB1, and phenol were, respectively, 392, 65, 49, and 20. The $K_L C_i$ value of adsorption on MB is in the hundreds,

Table 4
Separation factor and Favorable parameter

R_L value	$K_L C_i$ value	Type of process
$R_L > 1$	$K_L C_i < 0$	Unfavorable
$0 < R_L < 1$	$K_L C_i > 0$	Favorable
$R_L = 0$	$K_L C_i \to \infty$	Irreversible

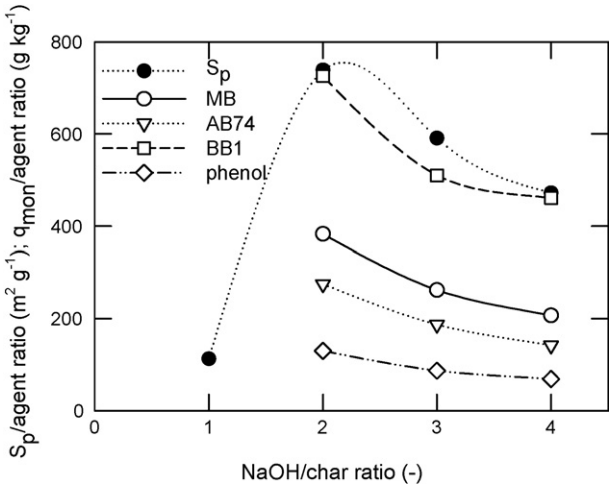

Fig. 8. Plot of q_{mon}/agent ratio and S_p/agent ratio against NaOH/char ratio of NaOH-activated carbon (adsorbates are MB (◯), AB74 (▽), BB1 (□), and phenol (◊), respectively).

and therefore extremely Favorable; adsorption on AB74, BB1, and phenol are in the tens, therefore highly Favorable; if $K_L C_i$ value is a single digit, then it is Favorable; if it is a decimal, it is weakly Favorable. Judging the Favorable level is of great significance for engineering applications. In this study, the $K_L C_i$ values of the adsorption of PKN2, PKN3, and PKN4 on certain adsorbates are close, meaning they are of similar adsorption type and highly Favorable.

3.6. Evaluation of activated carbon

For activated carbon preparation, the main cost lies in the consumption of the activation agent. Thus, the activation agent that produces the highest surface area per unit weight is the most economical. Surface area obtained per unit activation agent (S_P/agent ratio) of PKN2 in Fig. 8 is the highest. Porosity, micropore ratio, and burn-off of PKN2 is the lowest and bulk density of it, the highest, among the high surface area activated carbons (PKN2, PKN3, and PKN4). This means that PKN2 is of higher mass transfer efficiency, higher yield, and higher mechanical strength. Content of element C of PKN2 is higher, meeting the chemical property of good activated carbon [29]. The adsorption amounts per unit agent on four different adsorbates of PKN2 as shown in Fig. 8 are the highest. Favorable levels of PKN2 on four kinds of adsorbates are ether highly or extremely favorable.

4. Conclusions

Activated carbon prepared from the char of plum kernels using NaOH activation were studied. Microporous activated carbon with a surface area from 1478 to 1887 m^2 g^{-1} were obtained at a NaOH/char ratio from 2 to 4. According to the pore characteristics and SEM observation, it was inferred that there were two kinds of activation mechanisms: surface pyrolysis (NaOH/char ratio from 0 to 1) of stage 1 activated carbon; chemical etching and swelling (NaOH/char ratio from 2 to 4) of stage 2 activated carbon. According to elemental analysis and temperature

programmed desorption, it was inferred that the increased loss ratio of element O at a NaOH/char ratio from 1 to 2 is the key reason for swelling of stage 2 activated carbon, the reaction being according to formulas (2) and (3). Data obtained from isotherm equilibrium adsorption on dyes (MB, BB1, and AB74) and phenol suitably fitted the Langmuir isothermal equation; and the type of adsorption process was judged according to separation factor (R_L) and Favorable parameter ($K_L C_i$ value) as either extremely or highly favorable. Guidelines for evaluating chemically activated carbon for potential application were suggested. Activated carbon PKN2 in this study has these special characteristics and can be recommended as economical and environmentally friendly activated carbon.

Acknowledgment

Financial support for this work by the National Science Council, Taiwan, under Grant NSC95-2221-E-239-022 is gratefully acknowledged.

References

[1] F.C. Wu, R.L. Tseng, R.S. Juang, Preparation of highly microporous carbons from fir wood by KOH activation for adsorption of dyes and phenols from water, Sep. Purif. Technol. 47 (2005) 10–19.
[2] R.L. Tseng, S.K. Tseng, Pore structure and adsorption performance of the KOH-activated carbons prepared from corncob, J. Colloid Interface Sci. 287 (2005) 428–437.
[3] G.H. Oh, C.R. Park, Preparation and characteristics of rice-straw-based porous carbons with high adsorption capacity, Fuel 81 (2002) 327–336.
[4] W.T. Tsai, C.Y. Chang, S.L. Lee, A low cost adsorbens from agricultural waste corn cob by zinc chloride activation, Bioresour. Technol. 64 (1998) 211–217.
[5] C. Moreno-Castilla, F. Carrasco-Marin, M.V. Lopez-Ramon, M.A. Alvarez-Merino, Chemical and physical activation of olive-mill waste water to produce activated carbon, Carbon 39 (2001) 1415–1420.
[6] M. Molina-Sabio, F. Rodriguez-Reinoso, F. Caturla, M.J. Selles, Development of porosity in combined phosphoric acid–carbon dioxide activation, Carbon 34 (1996) 457–462.
[7] F.C. Wu, R.L. Tseng, C.C. Hu, C.C. Wang, The capacitive characteristics of activated carbons-comparisons of the activation method on the pore structure and effects of the pore structure and electrolyte on the capacitive performance, J. Power Sources 144 (2005) 302–309.
[8] M.A. Lillo-Rodenas, D. Logano-Castello, D. Cazorla-Amoros, A. Linares-Solano, Preparation of activated carbons from Spanish anthracite II. Activation by NaOH, Carbon 39 (2001) 751–759.
[9] S. Mitani, S.I. Lee, S.H. Yoon, Y. Korai, I. Mochida, Activation of raw pitch coke with alkali hydroxide to prepare high performance carbon for electric double layer capacitor, J. Power Sources 133 (2004) 298–301.
[10] A. Perrin, A. Celzard, A. Albiniak, J. Kaczmarczyk, J.F. Mareche, G. Furdin, NaOH activation of anthracites: effect of temperature on pore textures and methane storage ability, Carbon 42 (2004) 2855–2866.
[11] M.A. Lillo-Rodenas, J. Juan-Juan, D. Cazorla-Amoros, A. Linares-Solano, About reactions occurring during chemical activation with hydroxides, Carbon 42 (2004) 1365–1369.
[12] J.M. Macia-Agullo, B.C. Moore, D. Cazorla-Amoros, A. Linares-Solano, Activation of coal tar pitch carbon fibres: physical activation vs. chemical activation, Carbon 42 (2004) 1361–1364.
[13] A. Perrin, A. Celzard, A. Albiniak, M. Jasienko-Halat, J.F. Mareche, G. Furdin, NaOH activation of anthracites: effect of hydroxide content on pore textures and methane storage ability, Microporous Mesoporous Mater. 81 (2005) 31–40.
[14] F.C. Wu, R.L. Tseng, R.S. Juang, Pore structure and adsorption performance of the activated carbons prepared from plum kernels, J. Hazard. Mater. 69 (1999) 287–302.
[15] R.S. Juang, F.C. Wu, R.L. Tseng, Mechanism of adsorption of dyes and phenols from water using activated carbons prepared from plum kernels, J. Colloid Interface Sci. 227 (2000) 437–444.
[16] E.P. Barrett, L.G. Joyner, P.P. Halenda, The determination of pore volume and area distribution in porous substances. I. Computation from nitrogen isotherms, J. Am. Chem. Soc. 73 (1951) 373–380.
[17] J.H. de Boer, B.C. Lippens, B.G. Linsen, J.C.P. Broekhoff, A. van den Heuvel, T.J. Osiga, The *t*-curve of multimolecular N_2-adsorption, J. Colloid Interface Sci. 21 (1966) 405–414.
[18] K.S.W. Sing, D.H. Everett, R.A.W. Haul, L. Moscou, R.A. Pierotti, J. Rouquerol, Reporting physisorption data for gas/solid systems with special reference to the determination of surface area and porosity, Pure Appl. Chem. 57 (1985) 603–619.
[19] E.F. Sousa-Aguilar, A. Liebsch, B.C. Chaves, A.F. Costa, Influence of external surface area of small crystallite zeolites on the micropore volume determination, Microporous Mesoporous Mater. 25 (1998) 185–192.
[20] R.L. Tseng, F.C. Wu, R.S. Juang, Liquid-phase adsorption of dyes and phenols using pinewood-based activated carbons, Carbons 41 (2003) 487–495.
[21] F.C. Wu, R.L. Tseng, C.C. Hu, Comparisons of properties and adsorption performance of KOH-activated and steam-activated carbons, Microporous Mesoporous Mater. 80 (2005) 95–106.
[22] A.A. El-Hendawy, S.E. Samra, B.S. Girgis, Adsorption characteristics of activated carbons obtained from corncobs, Colloids Surf. A180 (2001) 209–221.
[23] M. Suzuki, Adsorption Engineering, Kodansha Ltd., Tokyo and Elsevier Science Publishers B.V., Amsterdam, 1990.
[24] M.A. Lillo-Rodenas, D. Cazoria-Amoros, A. Linares-Solano, Understanding chemical reactions between carbons and NaOH and KOH an insight into the chemical activation mechanism, Carbon 41 (2003) 267–275.
[25] K. Kinoshita, Carbon, in: Electrochemical and Physicochemical Properties, John-Wiley & Sons, New York, 1988.
[26] P.Z. Cheng, H. Teng, Electrochemical responses from surface oxide present on HNO_3 treated carbons, Carbon 41 (2003) 2057–2063.
[27] Y. Otake, R.G. Jenkins, Characterization of oxygen-containing surface complexes created on a microporous carbon by air and nitric acid treatment, Carbon 31 (1993) 109–121.
[28] G. McKay, Adsorption of dyestuffs from aqueous solutions with activated carbon. I. Equilibrium and batch contact time studies, J. Chem. Technol. Biotechnol. 32 (1982) 759–772.
[29] K. Gergova, N. Petrov, V. Minkova, A comparison of adsorption characteristics of various activated carbons, J. Chem. Technol. Biotechnol. 56 (1993) 77–82.